Isotope effects in inelastic 1.5-keV He^+-(H_2,D_2) collisions

A. L. Goldberger, D. H. Jaecks, M. Natarajan, and L. Fornari*
Behlen Laboratory of Physics, University of Nebraska, Lincoln, Nebraska 68588-0111
(Received 27 June 1983)

Linear- and circular-polarization measurements have been made for the $3\,^3P \rightarrow 2\,^3S$ transitions in helium resulting from the collision processes, $He^+ + H_2/D_2 \rightarrow He(3\,^3P) + H_2^+/D_2^+$. This was carried out at an incident-ion lab energy of 1.5 keV and for laboratory scattering angles ranging from 0.50 to 2.33 deg. The behavior of linear polarization for H_2 and D_2 targets as a function of scattering angle was found to be different, contrary to what one would expect from simple models that depend only upon the electronic structure of the system. Some correlation of the circular polarization between the two isotopes was found.

I. INTRODUCTION

The last decade has shown a marked increase in the utilization of polarized photon-scattered particle coincidence measurements to elucidate mechanisms in inelastic ion-atom collision processes.[1] From measurements of P-state excitation, one can often determine the magnetic substate cross sections $\sigma(M_L)$, and the phase differences $\Delta\phi$ of the associated scattering amplitudes.[2] Such results have shed new light on excitation processes since the observed radiation from the final state can be associated with the relative populations of the intermediate states of the temporary molecule formed during the collision.[3] The analysis of such photon-correlation data, within the context of the independent electron model has been particularly fruitful.

The use of polarized photon-scattered particle correlation measurements to study inelastic processes in ion-atom—molecule collisions has been more recent.[4–6] Owing to the added degrees of internal freedom of the molecule, the physical interpretation of the measured properties of the emitted radiation, in terms of collision mechanisms, is considerably more difficult than in the ion-atom case. Despite this difficulty, new insights into the collision process have begun to emerge.[7,8]

We report here on photon-correlation measurements at 1.5-keV incident ion energy of the process $He^+ + H_2/D_2 \rightarrow He(3\,^3P) + H_2^+/D_2^+$ that make direct comparisons between the two isotopes. Electronically, the two target systems are the same, and any differences in the cross sections for the two targets should result from differences in mass, the rotational and/or vibrational structure. In the region of the reported incident ion energy, the collision time is small compared to the typical vibrational and rotational frequencies.

II. EXPERIMENT

The experimental apparatus used for the present measurements has been discussed in earlier publications.[4,9] A 1.5-keV He^+ ion beam is incident on a target gas jet of H_2 (or D_2). The 3889-Å radiation from the $3\,^3P \rightarrow 2\,^3S$ transition of He is detected in a direction perpendicular to the collision plane; the collision plane being defined by the initial He^+ momentum and the final $He(2\,^3S)$ momentum. Delayed coincidence measurements between the 3889-Å radiation of a specific polarization and the scattered $He(2\,^3S)$ are made for laboratory scattering angles, varying between 0.50 and 2.33 deg. Circular-polarization measurements are made by inserting a quarter-wave plate before analyzing the polarization. The number of coincidences is normalized to the number of scattered neutral particles, thus minimizing errors introduced by fluctuations in ion beam intensity and scattering gas density. It should be noted that no analysis is done on the initial- or final-state distribution of the targets H_2/D_2.

Examples of typical sets of linear polarization data are shown in the polar plots of the radiation intensity for four specific linear polarization angles, at selected $He(2\,^3S)$ scattering angles (see Fig. 1).

III. RADIATION MEASUREMENTS

Our task in this section is to relate the measured radiation characteristics to atomic source parameters. There are several ways that this can be done. However, one would like to choose a representation that could possibly

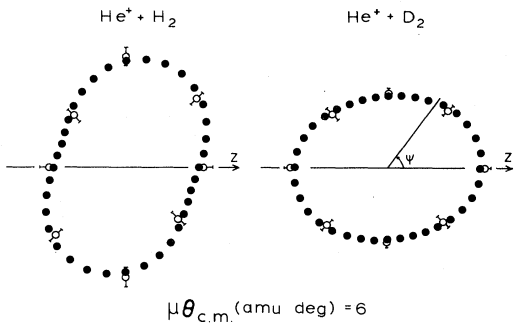

FIG. 1. Polar plots of the linear intensity $I(\psi)$ for H_2 and D_2 at two different scattering angles. The white circles with error bars are data, and the solid circles without error bars are least-squares fits of the data to Eq. (7).

lead to insights into the excitation mechanisms of the collision process. In the case of ion-atom collisions, this is often easy in that a one-to-one correspondence exists between the temporal molecular state quantum numbers to those of the final radiating atomic states. In the case of ion-atom—molecule collisions, the molecular states of the temporal three-particle complex are generally not known.

In an attempt to extend and relate our knowledge and understanding of binary systems to the three heavy-particle collision systems, we have chosen to represent measured polarization intensities in terms of the relative population of the magnetic sublevels of the $3\,^3P$ state.

The ensemble of atoms in a single "pure" state formed by a collision, can be represented by a single wave function. When more than one state of the total system (target plus projectile) is accessible, such as in the present $He^+ + H_2/D_2$ systems, then the ensemble is characterized by a weighted incoherent superposition of pure states.[10] The radiation from such an ensemble of excited atoms can be expressed in terms of alignment and orientation parameters, where the components represent average values over the ensemble.[11,12]

The intensity of this radiation measured in the detector frame is[11,12]

$$I=\tfrac{1}{3}CS[\,1-h^{[2]}G^{[2]}(A_0^{\rm det}-3A_{2+}^{\rm det}\cos2\beta) + \tfrac{3}{2}h^{[1]}G^{[1]}O_0^{\rm det}\sin2\beta]\,, \tag{1}$$

where C and S are constants; β describes the polarization, with $\beta=0,\pm\pi/4$ for linear, left, and right circularly polarized light, respectively. $A_0^{\rm det}$, $A_{2+}^{\rm det}$, and $O_0^{\rm det}$ are the components of the alignment and orientation parameters as measured in the detector frame. $G^{[k]}$ is a time-averaged expression accounting for the depolarization of light due to the fine-structure interaction. For the $3\,^3P\rightarrow 2\,^3S$ transition in helium, $h^{[1]}=2$, $h^{[2]}=-2$, $G^{[1]}=\frac{1}{2}$, and $G^{[2]}=\frac{5}{18}$.

The alignment and orientation parameters in Eq. (1) are defined in terms of the expectation values of the state multipoles.[11] They are related to the intrinsic properties of the radiation source and are a function of the angular coordinates of the photon detector. With the detector along the $+Y$ axis ($\theta=\phi=\pi/2$), the intensity of the linear radiation ($\beta=0$) can be expressed:

$$I=\tfrac{1}{3}CS[\,1+h^{[2]}G^{[2]}A_0^{\rm col}-\tfrac{3}{2}h^{[2]}G^{[2]}(A_0^{\rm col}-A_{2+}^{\rm col})\sin^2\psi + \tfrac{3}{2}h^{[2]}G^{[2]}A_{1+}^{\rm col}\sin2\psi]\,, \tag{2}$$

where

$$A_{11}=\langle L_xL_y+L_zL_y\rangle/L(L+1)\,,$$

$$A_0=\langle 3L_z^2-L^2\rangle/L(L+1)\,,$$

$$A_{2+}=\langle L_x^2-L_y^2\rangle/L(L+1)\,,$$

of the source.

The resulting polarization intensities can also be described in terms of the set of Stokes parameters, P_1,P_2,P_3, defined by[13]

$$P_1=\frac{I(0,0)-I(90,0)}{I(0,0)+I(90,0)}\,,$$

$$P_2=\frac{I(45,0)-I(135,0)}{I(45,0)+I(135,0)}\,, \tag{3}$$

$$P_3=\frac{I(45,90)-I(135,90)}{I(45,90)+I(135,90)}\,,$$

where $I(\psi,\alpha)$ is the intensity of the radiation polarized along a direction ψ, measured, in this case, with respect to the beam axis, and α is an added phase shift before the intensity is measured.

The parameter P_3 is often called the degree of circular polarization. Positive P_3 corresponds to right-hand circular polarization and a negative value to a left-hand circular polarization.

In terms of the alignment and orientation parameters,

$$P_1=\frac{3h^{[2]}G^{[2]}(A_0^{\rm col}-A_{2+}^{\rm col})}{4+h^{[2]}G^{[2]}(A_0^{\rm col}+3A_{2+}^{\rm col})}\,,$$

$$P_2=\frac{6h^{[2]}G^{[2]}A_{1+}^{\rm col}}{4+h^{[2]}G^{[2]}(A_0^{\rm col}+3A_{2+}^{\rm col})}\,, \tag{4}$$

$$P_3=\frac{6h^{[1]}G^{[1]}O_{1-}^{\rm col}}{4+h^{[2]}G^{[2]}(A_0^{\rm col}+3A_{2+}^{\rm col})}\,.$$

Because more than one final state of the collisional system (target plus projectile) is accessible, such as we would expect for the He^+-H_2/D_2 systems, the resulting Stokes parameters P_n are the sum of the parameters characterizing the radiation from each pure state i,[14]

$$P_n=\sum_i P_n^i\,, \tag{5}$$

where each final pure state will be represented by a collection of quantum numbers given by i. Included in this collection are the various possible initial- and final-state rotational and vibrational quantum numbers of the H_2/D_2 and $H_2{}^+/D_2{}^+$ molecule.

Experimental results for collision systems are often given in terms of the alignment and orientation parameters.[6] However, we prefer to present our results using Stokes parameters and interpret the results in terms of magnetic substate populations and their relative phases. Since the spin-orbit interaction in He is weak, the $3\,^3P$ state can be constructed from linear combinations of the orbital angular momentum eigenstates in the uncoupled representation. Assuming reflection symmetry, the correct quantum-mechanical expression for the linear polarization of the radiation emitted perpendicular to the scattering plane for a single final state of the collisional system in He($3\,^3P\rightarrow 2\,^3S$) transitions can be written[9]

$$I^i(\psi)=C_i[(28\sigma_0^i+26\sigma_1^i)+(30\sigma_1^i-15\sigma_0^i)\sin^2\psi + 15(2\sigma_0^i\sigma_1^i)^{1/2}\cos(\Delta\phi^i)\sin2\psi]\,. \tag{6}$$

$I^i(\psi)$ represents the intensity of radiation from the ith pure state. σ_0^i and σ_1^i are the differential cross sections for exciting the $m_L=0$ and ±1 magnetic sublevels of the ith pure state, respectively, and $\Delta\phi^i$ is the phase angle between the scattering amplitudes for $m_L=0$ and ±1 excitation of

the ith pure state. The constant C_i incorporates the relative weighing factor for each state.

The resulting linear intensity from an incoherent superposition of pure states is then

$$I(\psi)=\sum_i I_n^i(\psi)=A+B\sin^2\psi+C\sin 2\psi\ , \tag{7}$$

where n represents the collection of relevant quantum variables and the final momentum of the scattered particle for each pure state and A,B,C are functions of σ_0,σ_1.

The Stokes parameters can now be expressed in terms of the magnetic substate scattering cross sections:

$$P_1=\frac{k\sum_i(\sigma_0^i-2\sigma_1^i)}{\sum_i(\sigma_0^i+2\sigma_1^i)}\equiv k\frac{\sigma(0)-2\sigma(1)}{\sigma(0)+2\sigma(1)}\ ,$$

$$P_2=\frac{k\sum_i(2\sigma_0^i\sigma_1^i)^{1/2}\cos(\Delta\phi^i)}{\sum_i(\sigma_0^i+2\sigma_1^i)}\ , \tag{8}$$

$$P_3=\frac{k'\sum_i(2\sigma_0^i\sigma_1^i)^{1/2}\sin(\Delta\phi^i)}{\sum_i(\sigma_0^i+2\sigma_1^i)}\ .$$

k and k' depend on the particular transition. For the $He(3\,^3P\rightarrow 2\,^3S)$ transition, $k=15/41$ and $k'=27/41$.

The degree of polarization,[13] expressed in terms of these normalized Stokes parameters, is given by

$$P^2=(P_1/k)^2+(P_2/k)^2+(P_2/k')^2=(I_{\rm pol}/I_{\rm tot})^2\ . \tag{9}$$

When a single final state is observed with a single phase $\Delta\phi^i$, the above expression reduces identically to the coherency condition: $P^2=1$. The coherency matrix P, then, is the ratio of the intensity of polarized light to the total intensity. For completely coherent radiation, $|P|=1$.

Using Eq. (8), the coherency matrix can be written

$$P^2=1-4\sum_{i<j}\sum_{i<j}\frac{2\sigma_1^i\sigma_0^j+2\sigma_1^j\sigma_0^i-2(2\sigma_1^i\sigma_0^j)(2\sigma_1^j\sigma_0^i)\cos(\Delta\phi^i-\Delta\phi^j)}{\left[\sum_i(\sigma_0^i+2\sigma_1^i)\right]^2}\ . \tag{10}$$

In general $P^2<1$, since the sum is a positive quantity. However, the condition of complete coherence ($P^2=1$) can be met if $\Delta\phi^i=\Delta\phi^j$ and $\sigma_0^i/\sigma_1^i=\sigma_0^j/\sigma_1^j$. That is, the coherency condition is satisfied when the phase differences in each possible final state are the same and when the overall intensities from each pure state of the statistical distributions differ from each other by a multiplicative constant. A statement that $|P|=1$, when many final states are accessible, implies that the excitation to $He(3\,^3P)$ is independent of the state variables of the collisional partner or that only one state takes part in the reaction. This seemingly trivial result will later allow us to make statements about the collision process.

IV. EXPERIMENTAL RESULTS

In comparing the experimental differences between the H_2 and D_2 targets, one has a difficulty in deciding what physical variables should be chosen. Using the past results of ion-atom collisions as a guide, the relative velocity of the projectile target should be an important variable; therefore, we have performed all our measurements at the same laboratory energy.

Comparisons of differential (in angle) measurements are considerably more difficult because the exact form of the scattering potential is not known. For the same c.m. scattering angle, different regions of the interaction potential are probed depending upon the state of the target. Again, using the binary systems as a guide, we can attempt some comparisons. The classical c.m. scattering angle $\theta_{\rm c.m.}$ for a given relative velocity v and reduced mass μ can be written in terms of the classical impact parameter ρ and the interaction potential $V(r)$ (assuming a central potential and small scattering angles):

$$\theta_{\rm c.m.}=\frac{\rho}{\frac{1}{2}\mu v^2}\int_\rho^\infty\frac{dV(r)}{dr}\frac{dr}{(r^2-\rho^2)^{1/2}}\ . \tag{11}$$

If we wish to compare scattering that probes the same region of the potential, we compare data for the same impact parameter ρ; thus we plot our comparative H_2/D_2 data relative to $\mu\theta_{\rm c.m.}$.

For large impact parameters and some target orientations in which a central potential assumption is valid, this result should hold. Results of our measurements of the linear polarization in 1.5-keV $He^+ + H_2$ and $He^+ + D_2$ collisions for selected laboratory scattering angles are shown in Fig. 1. At each scattering angle, the coincidence rate is measured at four polarizer settings, and the intensity distribution is obtained by a best least-squares fit of the data to Eq. (7).

The measured values of P_1, P_2, and P_3 as a function of $\mu\theta_{\rm c.m.}$ are shown in Figs. 2, 3, and 4, respectively. The re-

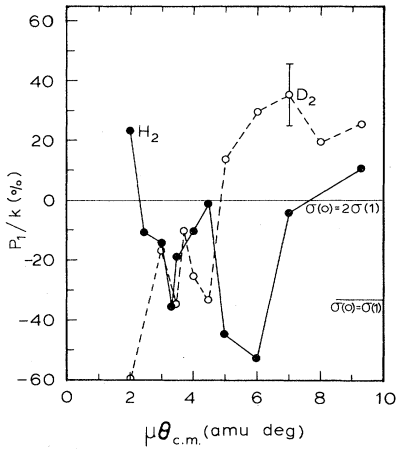

FIG. 2. Stokes parameter P_1/k for $He(3\,^3P)$ resulting from He^+-(H_2,D_2) collisions for selected values of $\mu\theta_{\rm c.m.}$.

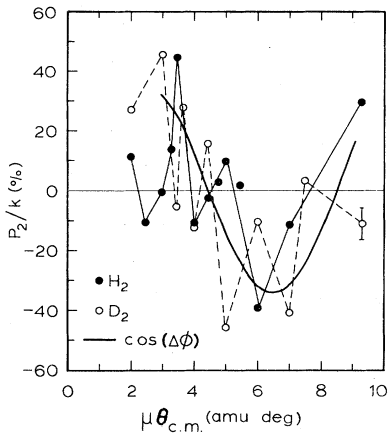

FIG. 3. Stokes parameter P_2/k for He($3\,^3P$) resulting from He^+-(H_2,D_2) collisions for selected values of $\mu\theta_{c.m.}$.

sulting values of the polarization $|P|$ are shown in Fig. 5. P_1 and P_2 are seen to vary rapidly with $\mu\theta_{c.m.}$, while the change in P_3 is less abrupt. It is clear that the behavior of P_1 is distinctly different for the two targets. P_3, the degree of circular polarization, can be seen to change from left-handed to right-handed with increasing $\mu\theta_{c.m.}$ angle for both H_2 and D_2. This occurs at the same "impact parameter" for both isotopes.

To accentuate further the difference between the H_2 and D_2 targets, we compare the electron charge distributions of the He($3\,^3P$) formed in the collision. From measured values of P_1, as shown in Fig. 2, it is clear that the shape of the electron cloud around the excited He is different for the two targets. For $\mu\theta_{c.m.}=6$ scattering, $\sigma(0)=0.66\sigma(1)$ for H_2 while for the same value of $\mu\theta_{c.m.}$, $\sigma(0)=4.15\sigma(1)$ for D_2.

The probability for total He($3\,^3P$) excitation as a function of $\mu\theta_{c.m.}$ is shown in Fig. 6. To make certain that the structure in the total probability of D_2 is real, we show two sets of total intensity measurements. The linear measurements are $I(0,0)+I(90,0)$, the denominator of P_1, and $I(45,90)+I(135,90)$, the denominator of P_3. By comparing the linear and circular polarization measurements, we find that the quarter-wave plate transmission to be 87.2%. The probability can be seen to increase with

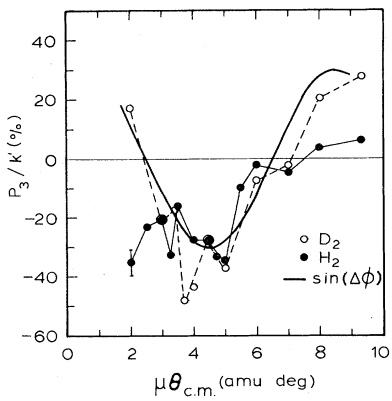

FIG. 4. Stokes parameter P_3/k' for He($3\,^3P$) resulting from He^+-(H_2,D_2) collisions for selected values of $\mu\theta_{c.m.}$.

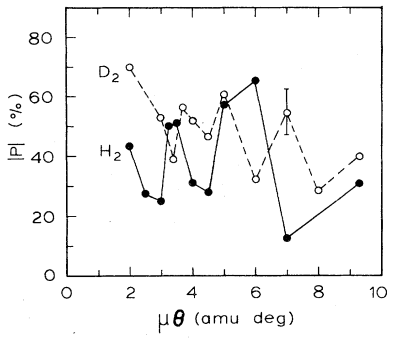

FIG. 5. Degree of polarization $|P|$ for He($3\,^3P$) resulting from He^+-(H_2,D_2) collisions at selected values of $\mu\theta_{c.m.}$.

scattering angle, but is larger for D_2 at all values but one of $\mu\theta_{c.m.}$ studied. The probability for scattering from D_2 also shows some oscillatory structure not present in H_2.

V. DISCUSSION

One striking feature of the experimental data is the agreement of P_3 between the two isotopes, as shown in Fig. 4, while P_1, as indicated in Fig. 2, shows little, if any, such correlation. This is because P_1 and P_3 reflect different properties of the He($3\,^3P$) and in turn are sensitive to different aspects of the collision process.

If we consider Eq. (11), we note that the values of P_3 for the two isotopes are approximately the same for equal values of $\mu\theta_{c.m.}=m_1\theta_{lab}$ over the range of 3–8 amu deg, where m_1 is the projectile mass. If the inelastic processes, measured as a function of θ_{lab}, behaved as small-angle potential scattering, P_1, P_2, and P_3 should be independent of target mass. Experiments by Rille *et al.*[15] verify this for H^+/D^+-H/D elastic collisions.

Considering Eq. (8), we note that P_3 is dominated by the $\sin(\Delta\phi^i)$ terms and is clearly the reason why P_3 is negative over a range of $\mu\theta_{c.m.}$. The denominator, $\sum_i(\sigma_0^i+2\sigma_1^i)$, is a more or less uniformly increasing function of $\mu\theta_{c.m.}$ as indicated by the total probability behavior, and thus will not dominate the behavior of P_3. Because of the rather high degree of coherence, as indicat-

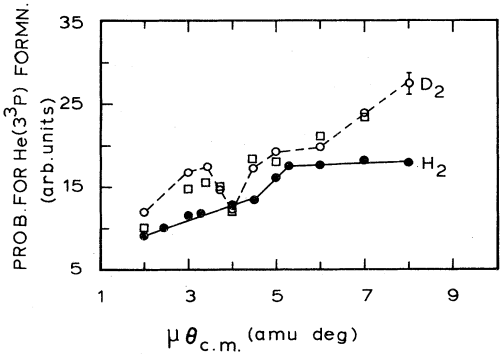

FIG. 6. Probability for He($3\,^3P$) formation in He^+-(H_2,D_2) collisions at selected values of $\mu\theta_{c.m.}$. Open circles and open squares for D_2 represent the probability computed from linear and circular polarization measurements, respectively.

ed by the values of $|P|$ around 40—50%, the sum $\sum_i (2\sigma_0^i\sigma_1^i)^{1/2}\sin(\Delta\phi^i)$ is dominated by one phase difference of the scattering amplitudes. The experimental results of P_3 suggest that this phase is the same for H_2 and D_2 at the same impact parameter.

The results of P_2, as shown in Fig. 3, also indicate the dominance of the $\cos(\Delta\phi^i)$ term. To more clearly show the effect of the $\sin(\Delta\phi)$ and $\cos(\Delta\phi)$ terms we have superimposed over P_3 and P_2 these functions. Note that when the $\sin(\Delta\phi)$ term is a minimum at about $\mu\theta_{\text{c.m.}}=4.50$ the $\cos(\Delta\phi)$ term is going through zero as it should. Variations in P_3 and P_2 about these two functions are primarily due to the variations in the coefficients, $(2\sigma_0^i\sigma_1^i)^{1/2}$. To further elucidate this effect we have plotted $\sigma(0)$ and $\sigma(1)$ separately in Fig. 7 as obtained from the measured values of P_1. We note that the principal difference in P_3 at 6—9 amu deg is the result of the increased value of $\sigma(0)$ for D_2 over that for H_2. From Fig. 7, it is clear there is no apparent correlation in $\sigma(0)$ and $\sigma(1)$ when comparing the two isotopes, except some overall general increase in $\sigma(0)$ with increasing $\mu\theta_{\text{c.m.}}$.

Taulbjerg *et al.*[16] have derived a scaling law for rotational coupling, a possible mechanism for exciting σ_1 in the present systems. Although it is not clear whether the rotational coupling scaling law applies to the present system, we attempted to fit σ_1 for H_2 and D_2 to it. Their scaling law suggests that our present results should scale as $\theta_{\text{c.m.}}$ which was not found to be the case.

Our data suggest that the assumption of the fixed nucleus approximation that H_2 and D_2 are equivalent, for the inelastic process measured, is not a good one. One possible internal parameter of H_2 and D_2 that might affect the process is the initial population distribution of the rotational quantum numbers at room temperature. Summing contributions to the process over all fixed nucleus orientations is equivalent to summing over all magnetic substates M_N of any one possible rotational state N. If we allow for the possibility of interference from different orientations within any M_N state, one could obtain differences between the isotopes, since at room temperature, the rotational populations are distributed differently. This system merits further investigation so that the role of the internal H_2/D_2 variables can be explored, perhaps by carrying out the measurements with cooled targets or with cooled ortho- and parahydrogen separately.

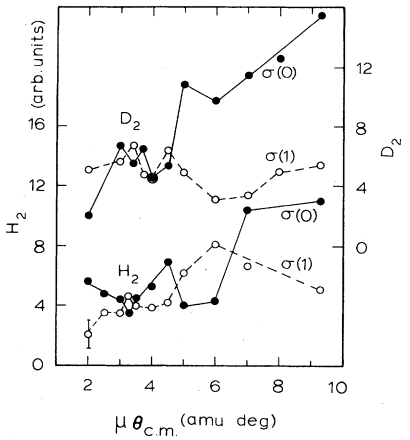

FIG. 7. Values of $\sigma(0)$ and $\sigma(1)$ formed in He^+—(H_2,D_2) collisions at selected values of $\mu\theta_{\text{c.m.}}$. Scales on the right and left correspond to D_2 and H_2, respectively.

VI. CONCLUSION

We can conclude that the fixed nucleus approximation is insufficient to explain the differences in H_2 and D_2, namely that the magnetic substate cross sections, $\sigma(0)$ and $\sigma(1)$, behave differently as functions of $\mu\theta_{\text{c.m.}}$, while the phase differences $\Delta\phi$ are rather similar. This suggests that the excitation mechanisms are the same for the two isotopic targets; however, the relative degree to which these mechanisms operate is different.

ACKNOWLEDGMENT

This work was supported by the National Science Foundation.

*Present address: L. Fornari, Department of Physics, University of Texas, Arlington, Texas, 76019.

[1]*Coherence and Correlations in Atomic Collisions,* edited by H. Kleinpoppen and J. F. Williams (Plenum, New York, 1980).
[2]J. Macek and D. H. Jaecks, Phys. Rev. A 4, 2288 (1971).
[3]D. H. Jaecks, A. L. Goldberger, M. Natarajan, D. Montgomery, and D. Mueller, in *Physics of Electronic and Atomic Collisions,* edited by S. Datz (North-Holland, Amsterdam, 1982).
[4]F. J. Eriksen and D. H. Jaecks, Phys. Rev. A 17, 1296 (1978).
[5]W. Reiland, G. Jamieson, U. Tittes, and I. V. Hertel, Z. Phys. A 307, 51 (1982).
[6]K. H. Blattman, B. Menner, W. Schauble, B. Staudenmayer, L. Zehnle, and V. Kempter, J. Phys. B 13, 3635 (1980).
[7]D. H. Jaecks, O. Yenen, M. Natarajan, and D. Mueller, Phys. Rev. Lett. 50, 825 (1983).
[8]D. Dowek, D. Dhuicq, V. Sidis, and M. Barat, Phys. Rev. A 26, 746 (1982).
[9]F. J. Eriksen, D. H. Jaecks, W. deRijk, and J. Macek, Phys. Rev. A 14, 119 (1976).
[10]U. Fano, Rev. Mod. Phys. 29, 74 (1957).
[11]U. Fano and J. Macek, Rev. Mod. Phys. 45, 53 (1973).
[12]J. N. Gau and J. Macek, Phys. Rev. A 12, 1760 (1975).
[13]M. Born and E. Wolf, *Principles of Optics* (Pergamon, New York, 1970).
[14]S. Chandrasekhar, Astrophys. J. 105, 424 (1947).
[15]E. Rille, R. E. Olson, J. L. Peacher, D. M. Blankenship, T. J. Blankenship, T. J. Kvale, E. Read, and J. T. Park, Phys. Rev. Lett. 49, 1819 (1982).
[16]K. Taulberg, J. S. Briggs, and J. Vaaben, J. Phys. B 9, 1351 (1976).